Carrier-Envelope Phase-Dependent Strong-Field Excitation

D. Chetty,[1] R. D. Glover,[1,2] X. M. Tong,[3] B. A. deHarak,[1,4] H. Xu,[1] N. Haram,[1] K. Bartschat,[5] A. J. Palmer,[1] A. N. Luiten,[2] P. S. Light,[2] I. V. Litvinyuk,[1] and R. T. Sang[1,*]

[1]*Centre for Quantum Dynamics, Griffith University, Brisbane, Queensland 4111, Australia*
[2]*Institute for Photonics and Advanced Sensing and School of Physical Sciences, The University of Adelaide, Adelaide, South Australia 5005, Australia*
[3]*Center for Computational Sciences, University of Tsukuba, 1-1-1 Tennodai, Tsukuba, Ibaraki 305-8573, Japan*
[4]*Physics Department, Illinois Wesleyan University, Bloomington, Illinois 61702-2900, USA*
[5]*Department of Physics and Astronomy, Drake University, Des Moines, Iowa 50311, USA*

(Received 18 August 2021; accepted 15 March 2022; published 26 April 2022)

We present a joint experimental-theoretical study on the effect of the carrier-envelope phase (CEP) of a few-cycle pulse on the atomic excitation process. We focus on the excitation rates of argon at intensities in the transition between the multiphoton and tunneling regimes. Through numerical simulations, we show that the resulting bound-state population is highly sensitive to both the intensity and the CEP. The experimental data clearly agree with the theoretical prediction, and the results encourage the use of precisely tailored laser fields to coherently control the strong-field excitation process. We find a markedly different behavior for the CEP-dependent bound-state population at low and high intensities with a clear boundary, which we attribute to the transition from the multiphoton to the tunneling regime

DOI: 10.1103/PhysRevLett.128.173201

High-intensity lasers provide access to highly excited bound states that have a variety of applications. For example, excited states that decay directly to the ground state produce coherent EUV light through below-threshold harmonic (BTH) generation [1,2], and in noble gases long-lived metastable states may be populated, either directly or through cascade decay of higher states [3,4]. This offers an alternative excitation pathway for a variety of applications [5–9]. In this commonly referred to "strong-field regime," excitation mechanisms are typically explained using either the multiphoton (MP) or tunneling picture, with the Keldysh parameter γ [10] providing a measure for which one is most appropriate. In the MP regime ($\gamma \gg 1$), an excited state can be reached via the absorption of multiple photons whose energy add up. In the tunneling regime ($\gamma < 1$), excitation is the result of recapturing tunneled electrons, a process usually referred to as frustrated tunnel ionization [3]. In the intermediate regime ($\gamma \approx 1$), there is a rich variety of physics, as there are contributions from both MP and tunneling effects.

For few-cycle pulses, the carrier-envelope phase (CEP) becomes an important parameter for controlling interactions; for example, the CEP has been shown to play a crucial role in processes such as high-harmonic generation [11], above-threshold ionization [12], generation of attosecond pulses [13,14], coherent control of molecular dynamics [15,16], and control of BTH [17,18]. Because excitation is described very differently in the MP and tunneling regimes, it is expected that the effect of changing the CEP will manifest differently depending on the intensity. There are only a few studies to date that have explored how the CEP affects the final bound-state populations, particularly in the tunneling regime. The CEP can potentially be used to control populations or serve as a clear marker for the changing dynamics of the interaction from MP absorption to tunneling ionization plus recapture.

In this Letter, we analyze the effect of the CEP on strong-field excitation. We experimentally investigate excitation rates of argon as a function of CEP in the tunneling regime, where we find good agreement between our experimental data and numerical results based on the time-dependent Schrödinger equation (TDSE). We show that the bound-state population strongly depends on the CEP, especially in the tunneling regime where both the distribution of populated states and the total excitation rates are highly sensitive to the CEP. The TDSE results show that at lower laser intensities, intermediate between the MP and tunneling regimes, a remarkable change occurs in the dependence of the final bound-state populations on the CEP. The change in behavior indicates the transition of the dynamics from MP excitation to recaptured tunneling.

Excitation of atoms or molecules in the strong-field regime is unique. The laser field is comparable to the field strength between the outer electron(s) and the nucleus, and there are many different excitation pathways to a complex manifold of excited states. Furthermore, the energy levels are strongly modified due to the ac Stark shift, and the excitation probability to a particular target state will depend strongly on the intensity of the laser field [19–21]. Regularly spaced enhancements exist that depend on the

peak laser intensity [4,22–26]. In the MP picture, these enhancements occur when the ac Stark-shifted ionization threshold crosses the energy level of an integer number N of absorbed photons, known as channel closings [27,28]. Consequently, high-energy Rydberg states come into resonance at regularly spaced intensity intervals with $\Delta U_P(I) = \omega$, where $U_P = I/4\omega^2$ is the ponderomotive energy of the electron, I is the laser intensity, and ω is the laser frequency. (Unless indicated otherwise, we use atomic units throughout.) At higher intensities, where tunnel ionization dominates, excitation is more commonly described in the time domain. Here, enhancements in excitation rates are a result of constructive interference between electron wave packets emitted at subsequent field-cycle maxima, which are recaptured into the same quantum state [26,29]. In the strong-field approximation for sufficiently long pulses, electrons born one period T apart are launched in the same direction, and their subsequent dynamics are very similar. Their contributions to a particular state, however, differ by a phase $\Delta\theta = T(U_P + I_P + E_{nl})$. This leads to the condition for constructive interference as

$$m\omega = I_P + E_{nl} + U_P, \tag{1}$$

where m is a real integer, E_{nl} is the field-free energy of the nl orbital, and I_P is the static ionization potential. This closely resembles the condition in the MP regime with the same intensity interval between successive enhancements.

We have previously shown that enhancements are broadened for CEP-averaged few-cycle pulses [4]. In the MP picture, many resonance pathways exist, and, thus, an individual state may be reached through absorption of photons from any part of the frequency spectrum. Each pathway can be made up of a unique N that typically obeys the dipole selection rules [24,25,30–32]. If we consider the contribution due to nondipole transitions [33], it does not change the conclusions here, since the nondipole effect is negligibly small. The overall transition amplitude to a particular state is the coherent sum of the contributions from each pathway. In this picture, the CEP should have an effect only for off-resonance excitation [34–37].

In the tunneling picture, the CEP significantly alters the time dependence of the electric field. Consequently, the dynamics of electrons born at subsequent field-cycle maxima are no longer similar. In this case, the electron wave packets are born at different U_P, dependent on the CEP, and the condition for constructive interference given by Eq. (1) needs to be modified accordingly. Hence, the energy of the final state where constructive interference occurs will be modified, and it is expected that modifying the CEP, in turn, modifies the relative populations of the resulting bound states. This has been demonstrated indirectly through BTH [1,17,18] but has yet to be shown directly either experimentally or theoretically.

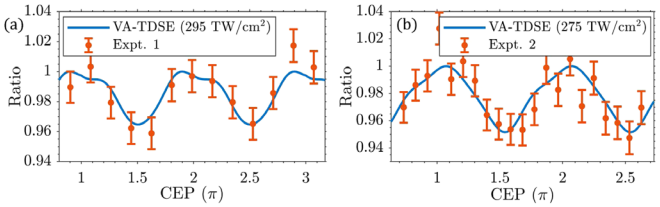

FIG. 1. Comparison of the experimentally measured ratio of excitation yields to ionization yields and the volume-averaged TDSE results for two datasets. The absolute phase (unknown; see the text) and normalized yield obtained in the experiment were shifted to best fit theory.

In our Letter, we measure excitation yields of argon resulting from the interaction with CEP-stabilized few-cycle laser pulses at peak intensities of 275 and 295 TW/cm^2. The experimental procedure and detection methods are described in Ref. [4]. Briefly, CEP-stabilized laser pulses are obtained from a commercial laser system (Femto Power Pro CE-Phase) with a pulse duration of ~6 fs (FWHM) centered at 800 nm. A commercial $f-2f$ interferometer (Menlo APS800) located close to the interaction region is integrated to compensate long-term drifts and measure the stability of the locking system. The CEP is locked to a fixed (though arbitrary, i.e., not absolutely known) value, while the relative shift is controlled by translation of a fused-silica wedge (1 mm ≈ 1.25 rad phase shift). To quantify excitation rates after interaction with the laser, we measure the yields of excited atoms (Ar^*) surviving a 0.15–0.6 ms flight time to a microchannel plate detector. Simultaneously, we detect ionization yields (Ar^+) using a time-of-flight apparatus to distinguish charged and neutral particles. The measured yield of (Ar^*) is expected to be proportional to the total yield summed over all n and l [38].

Two results of these measurements together with numerical simulations are shown in Fig. 1. Because the measurement requires that the experimental parameters remain stable, we are restricted to high intensities where the integration times are small enough to maintain a stable CEP lock. At peak intensities below ~250 TW/cm^2, long-term instability of the laser intensity dominates, and we are unable to resolve a CEP effect. We observe the ratio of Ar^*/Ar^+, as this removes experimental systematics such as the density of the atomic beam, which has a small but significant fluctuation. In both experiments, a clear modulation in the yields is observed with a similar level of modulation on the order of 5% and a period of π, as required by symmetry of the excitation process.

The comparison of the experimental measurements and the TDSE predictions (solid lines) shows very good agreement and gives us confidence that the numerical results are a good representation of the interaction process. The experimentally measured yields are affected by intensity-volume averaging (VA) and CEP fluctuations, and the numerical results have been processed to account for these.

(See Supplemental Material [39] for details, which includes Ref. [40].) The details of the calculations have been described elsewhere [4]. Briefly, they are based on solving the TDSE in the single-active-electron approximation by splitting the wave function into an inner and outer region. The outer wave function is projected onto momentum space, and the total ionization probabilities are obtained by integrating the electron momentum distribution over the entire momentum space. Quantum-state populations up to $n = 30$, $l = 29$ are found by projecting the inner-region wave function on the field-free atomic excited states. The total excitation probability $P(\mathrm{Ar}^*)$ is obtained by summing up all these populations.

We use the TDSE results to extend our study to lower intensities and compare the bound-state populations in the transition between the MP and tunneling regimes where we observe a clear change in behavior. Our previous work [4], which measured the bound-state yields over a broad intensity range, demonstrates that our theory is valid at the intensities investigated here. Figure 2(a) compares the total excitation probability for a cosine and sine pulse (CEP $= 0$ and 0.5π, respectively). At low intensity, the excitation probability for the sine pulse maximizes at a slightly lower intensity (in each channel-closing cycle) than for the cosine pulse. A clear change in this behavior occurs at $\sim$125 TW/cm^2 ($\gamma \sim 1$), where the order in which the peaks are observed is flipped and the intensity separation between them is increased to the point where the two curves become almost completely out of phase. This is clearly shown in the plot by the relative phase difference of the oscillations, $\Delta\sigma$, which exhibits a sharp change starting at $\sim$100 TW/cm^2 and eventually experiences a shift of close to $2\pi/3$. (See Supplemental Material [39] for details.) The clear modification in behavior in this region indicates the changing dynamics from the multiphoton to the tunneling regime. In the MP regime, the sine pulse leading the cosine pulse is consistent with observations of CEP effects using few-cycle rf pulses [41] and is due to the interference between different MP pathways. In the tunneling regime, the ponderomotive potential at the maximum of the field cycle is larger for the cosine pulse. Hence, the condition for constructive interference given in Eq. (1) is reached at a lower intensity compared to the sine pulse, and the cosine pulse is observed to lead the sine pulse. Because we already observe a difference in the ratio $\mathrm{Ar}^*/\mathrm{Ar}^+$ experimentally for sine and cosine pulses, albeit at a fixed intensity, we expect these oscillations to survive VA.

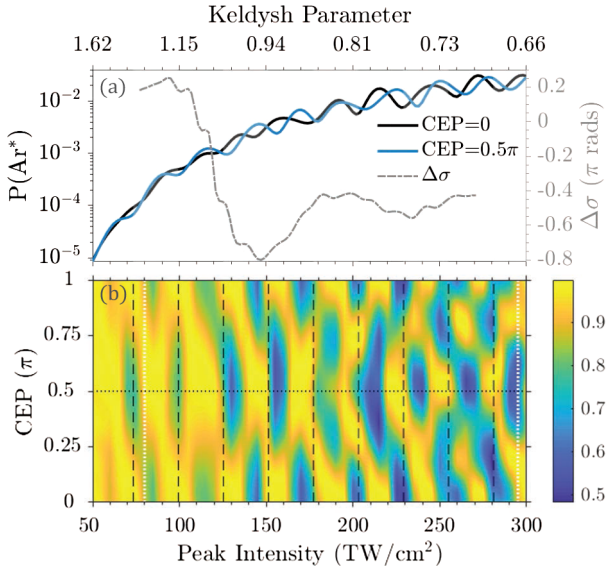

FIG. 2. (a) Total excitation probabilities from TDSE calculations as a function of intensity for a cosine and sine few-cycle pulse. The dashed line (referring to the right y scale) shows the relative phase difference of the observed oscillations. (b) Excitation probabilities as a function of CEP and intensity normalized to their respective maximum at each intensity. The dotted white lines correspond to lineouts shown in Fig. 4. The black dashed lines mark the 13- to 22-photon channel closings, and the shaded regions correspond to odd-photon absorption channels. No volume averaging was performed.

At the same intensity where the relative phase change is observed, we also notice an increase in the modulation depth when changing the CEP. Figure 2(b) shows the excitation probabilities for each intensity scaled to the maximum excitation probability at that intensity for all CEPs. Similar patterns repeat at a period close to that of the channel closings, and this pattern continues from the low-intensity to the high-intensity regime, where the conditions for both channel closings and the quantum trajectory model used to derive Eq. (1) explain this periodicity. It is clear that the sensitivity of the bound-state populations to the CEP is dependent on the intensity. Below the 15-photon channel closing ($\sim$125 TW/cm^2, $\gamma \sim 1$), the change in total excitation probability as a function of the CEP is approximately 20%. At higher intensities, there is a steplike increase to $>40\%$ in successive channels.

The distribution of l states after excitation has been studied previously both semiclassically [31] and quantum mechanically [24,25,29,30]. In the MP picture, excitation follows the dipole selection rules and for an argon atom, absorption of an even (odd) number of photons will preferentially populate odd (even) l's, which is referred to as odd (even) parity. A change in parity between odd and even is indicative of an additional absorbed photon. Previously, we showed that the parity effect is observed for CEP-averaged pulses [4]. Here, we investigate whether this is true for both sine and cosine pulses. The distribution of l states due to excitation from a cosine pulse is shown in Fig. 3(a) and a sine pulse in Fig. 3(b). Figure 3(c) shows the sum of the excitation probability over all odd and even l states. At low intensity, the parity effect is observed for both CEPs with excitation to odd (even) l occurring when an even (odd) number of photons are absorbed, consistent with the expectation from the MP model [31,42].

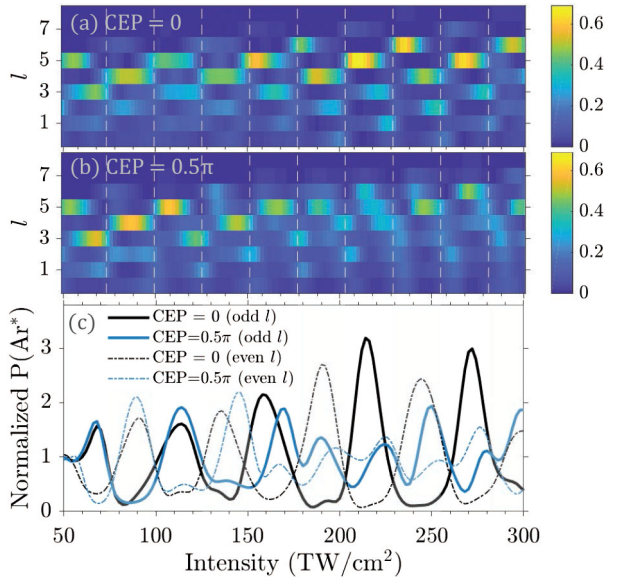

FIG. 3. (a) Normalized probability for excitation to different l states for a CEP = 0 (cosine) pulse. (b) As in (a) but for a CEP = 0.5π (sine) pulse. (c) Normalized probability for excitation to the sum of states with odd l (thick solid lines) and even l (thin dashed lines). The white dashed lines mark the 13- to 22-photon channel closings, and the shaded regions correspond to odd-photon absorption channels. No volume averaging was performed.

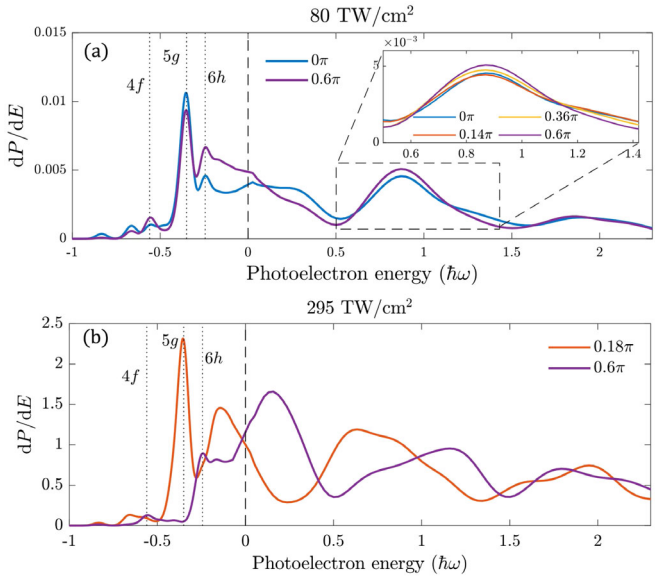

FIG. 4. Normalized excitation and ionization spectra for select CEPs at peak intensities of (a) 80 and (b) 295 TW/cm^2. The dashed line marks the shifted ionization potential, and the dotted lines mark the principal excited states. No volume averaging was performed.

For cosine pulses, we observe parity at all intensities investigated, with excitation to odd and even l's at successive n-photon absorption channels. However, for sine pulses at intensities beyond $\gamma \sim 1$, we show a clear loss of the parity effect. The population is spread across a range of quantum states with odd and even l's populated in each n-photon absorption channel. Venzke *et al.* [42] previously showed that the parity effect can break down with few-cycle pulses, where it was proposed to be a consequence of the bandwidth of the pulse. However, here we show that parity is observed in the low-intensity regime but depends on the CEP at higher intensities. The fact that parity is observed for a few-cycle cosine pulse suggests that the bandwidth of the pulse is not directly responsible for the loss of the parity effect. Thus, we attribute our observation to the breakdown of inversion symmetry of the electric field for a sine and cosine pulse. This is indicative of a transition in the excitation mechanism from the MP to the tunneling regime, since the spatial symmetry of the electric field should matter only in the tunneling-plus-recapturing excitation model.

Based on quantum defect theory [43–45], the photoexcitation and photoionization processes can be treated in a unified way in the perturbative limit. Recently, Gao and Tong [46] showed that such a relation still exists even in a nonperturbative regime. Figure 4 shows the normalized photoelectron spectra across the ionization threshold (negative energy stands for excitation) at 80 and 295 TW/cm^2, which lie before and far after the stepwise increase in modulation, respectively. We illustrate two CEPs that correspond to the minimum and maximum excitation yields. The lower intensity of 80 TW/cm^2 lies close to the 13-photon resonance to the $5g$ state. At this intensity, excitation to the $5g$ state and also to high-lying states near the continuum dominates the relative population. As the CEP is varied from 0 to 0.6π, there is a smooth change in the total number of bound-state electrons with a modulation depth of ~15%. When the total population is increased, the population of the $5g$ state is reduced. The change we observe in the structure of the bound-state spectrum is less significant in the low-energy photoelectron spectrum, as shown in the inset in Fig. 4(a).

In contrast, at 295 TW/cm^2 there is a drastic change of the bound-state spectrum and also the continuum peak structure when the CEP is varied. At this high intensity, both the structure and the positions of the peaks are significantly modified with the CEP, accounting for the high sensitivity in bound-state populations observed in Fig. 2(b). The populations of individual states are observed to be extremely CEP sensitive, with the population of the $5g$ state fluctuating from a maximum to effectively zero with changing CEP. However, comparing the CEP dependence at both intensities, one similarity is observed. It appears that maximum excitation occurs at a CEP that facilitates the transfer of near-zero momentum photoelectrons below the ionization threshold, resulting in a reduced number of small-momentum photoelectrons.

In conclusion, we experimentally demonstrated that bound-state populations are modified depending on the

CEP of the driving laser pulse. This serves as a proof of principle that bound-state populations can be controlled through precisely engineered pulses. We hope that our findings will encourage the use of other means such as two-color fields, which can be used for precisely controlling the electric field [47]. With such fields, it should be possible to coherently control bound-state populations in the same manner as via the CEP. We also predict that the CEP provides a unique method to explore the boundary between the MP and the tunneling regimes. Not only does the level of modulation of the excited-state populations increase in the tunneling regime, but we also observe more subtle effects: the change in relative phase of the peak structure in the intensity dependence and the loss of the parity effect for sine pulses. Both of these phenomena warrant further investigation with alternative experimental methods.

This project is supported under the Australian Research Council's Linkage Infrastructure, Equipment and Facilities scheme (Project No. LE160100027). D. C. is supported by an Australian Government RTP Scholarship. N. H. is supported by a Griffith University International Postgraduate Research Scholarship (GUIPRS), and H. X. is supported by an ARC Discovery Early Career Researcher Grant No. DE130101628. X-.M. T. was supported by Multidisciplinary Cooperative Research Program in CCS, University of Tsukuba. Further funding was provided by the United States National Science Foundation under Grants No. PHY-1402899 and No. PHY-1708108 (B. A. d. H.) as well as No. PHY-1803844 and No. PHY-2110023 (K. B.).

*r.sang@griffith.edu.au

[1] W.-H. Xiong, X.-R. Xiao, L.-Y. Peng, and Q. Gong, Phys. Rev. A **94**, 013417 (2016).
[2] Y. Zhao, Y. Zhou, J. Liang, Z. Zeng, Q. Ke, Y. Liu, M. Li, and P. Lu, Opt. Express **27**, 21689 (2019).
[3] T. Nubbemeyer, K. Gorling, A. Saenz, U. Eichmann, and W. Sandner, Phys. Rev. Lett. **101**, 233001 (2008).
[4] D. Chetty, R. D. Glover, B. A. deHarak, X. M. Tong, H. Xu, T. Pauly, N. Smith, K. R. Hamilton, K. Bartschat, J. P. Ziegel, N. Douguet, A. N. Luiten, P. S. Light, I. V. Litvinyuk, and R. T. Sang, Phys. Rev. A **101**, 053402 (2020).
[5] M. Baker, A. J. Palmer, W. R. MacGillivray, and R. T. Sang, Nanotechnology **15**, 1356 (2004).
[6] Z.-T. Lu, P. Schlosser, W. Smethie, N. Sturchio, T. Fischer, B. Kennedy, R. Purtschert, J. Severinghaus, D. Solomon, T. Tanhua *et al.*, Earth Sci. Rev. **138**, 196 (2014).
[7] N. C. Sturchio, K. L. Kuhlman, R. Yokochi, P. C. Probst, W. Jiang, Z.-T. Lu, P. Mueller, and G.-M. Yang, J. Contam. Hydrol. **160**, 12 (2014).
[8] A. Knecht, Z. Alexander, Y. Bagdasarova, T. Cope, B. Delbridge, X. Fléchard, A. García, R. Hong, E. Liénard, P. Mueller *et al.*, in *AIP Conference Proceedings* (AIP, New York, 2013), Vol. 1560, pp. 636–640, 10.1063/1.4826859.
[9] B. Ohayon, J. Chocron, T. Hirsh, A. Glick-Magid, Y. Mishnayot, I. Mukul, H. Rahangdale, S. Vaintraub, O. Heber, D. Gazit *et al.*, Hyperfine Interact. **239**, 57 (2018).
[10] L. V. Keldysh, Sov. Phys. JETP **47**, 1307 (1964).
[11] I. P. Christov, M. M. Murnane, and H. C. Kapteyn, Phys. Rev. Lett. **78**, 1251 (1997).
[12] C. Haworth, L. Chipperfield, J. Robinson, P. Knight, J. Marangos, and J. Tisch, Nat. Phys. **3**, 52 (2007).
[13] R. Kienberger, M. Hentschel, M. Uiberacker, C. Spielmann, M. Kitzler, A. Scrinzi, M. Wieland, T. Westerwalbesloh, U. Kleineberg, U. Heinzmann *et al.*, Science **297**, 1144 (2002).
[14] A. Baltuška, T. Udem, M. Uiberacker, M. Hentschel, E. Goulielmakis, C. Gohle, R. Holzwarth, V. Yakovlev, A. Scrinzi, T. W. Hänsch *et al.*, Nature (London) **421**, 611 (2003).
[15] V. R. Bhardwaj, S. A. Aseyev, M. Mehendale, G. L. Yudin, D. M. Villeneuve, D. M. Rayner, M. Y. Ivanov, and P. B. Corkum, Phys. Rev. Lett. **86**, 3522 (2001).
[16] H. Xu, T.-Y. Xu, F. He, D. Kielpinski, R. T. Sang, and I. V. Litvinyuk, Phys. Rev. A **89**, 041403(R) (2014).
[17] M. Chini, X. Wang, Y. Cheng, H. Wang, Y. Wu, E. Cunningham, P.-C. Li, J. Heslar, D. A. Telnov, S.-I. Chu *et al.*, Nat. Photonics **8**, 437 (2014).
[18] H. Yun, J. H. Mun, S. I. Hwang, S. B. Park, I. A. Ivanov, C. H. Nam, and K. T. Kim, Nat. Photonics **12**, 620 (2018).
[19] P. H. Bucksbaum, Phys. Today **57**, 58 (2004).
[20] H. Rabitz, R. de Vivie-Riedle, M. Motzkus, and K. Kompa, Science **288**, 824 (2000).
[21] A. Bunjac, D. B. Popović, and N. S. Simonović, Phys. Chem. Chem. Phys. **19**, 19829 (2017).
[22] H. Zimmermann, S. Patchkovskii, M. Ivanov, and U. Eichmann, Phys. Rev. Lett. **118**, 013003 (2017).
[23] Q. Li, X.-M. Tong, T. Morishita, C. Jin, H. Wei, and C. Lin, J. Phys. B **47**, 204019 (2014).
[24] Q. Li, X.-M. Tong, T. Morishita, H. Wei, and C. D. Lin, Phys. Rev. A **89**, 023421 (2014).
[25] B. Piraux, F. Mota-Furtado, P. F. O'Mahony, A. Galstyan, and Y. V. Popov, Phys. Rev. A **96**, 043403 (2017).
[26] S. P. Xu, M. Q. Liu, S. L. Hu, Z. Shu, W. Quan, Z. L. Xiao, Y. Zhou, M. Z. Wei, M. Zhao, R. P. Sun, Y. L. Wang, L. Q. Hua, C. Gong, X. Y. Lai, J. Chen, and X. J. Liu, Phys. Rev. A **102**, 043104 (2020).
[27] P. Kruit, J. Kimman, H. G. Muller, and M. J. V. der Wiel, J. Phys. B **16**, 937 (1983).
[28] H. G. Muller, A. Tip, and M. J. van der Wiel, J. Phys. B **16**, L679 (1983).
[29] S. Hu, X. Hao, H. Lv, M. Liu, T. Yang, H. Xu, M. Jin, D. Ding, Q. Li, W. Li *et al.*, Opt. Express **27**, 31629 (2019).
[30] Z. Chen, T. Morishita, A.-T. Le, M. Wickenhauser, X. M. Tong, and C. D. Lin, Phys. Rev. A **74**, 053405 (2006).
[31] D. G. Arbó, K. I. Dimitriou, E. Persson, and J. Burgdörfer, Phys. Rev. A **78**, 013406 (2008).
[32] K. Krajewska, I. I. Fabrikant, and A. F. Starace, Phys. Rev. A **86**, 053410 (2012).
[33] H. Ni, S. Brennecke, X. Gao, P.-L. He, S. Donsa, I. Březinová, F. He, J. Wu, M. Lein, X.-M. Tong, and J. Burgdörfer, Phys. Rev. Lett. **125**, 073202 (2020).

[34] T. Nakajima and S. Watanabe, Phys. Rev. Lett. **96**, 213001 (2006).
[35] T. Nakajima and S. Watanabe, Opt. Lett. **31**, 1920 (2006).
[36] D. Peng, B. Wu, P. Fu, B. Wang, J. Gong, and Z.-C. Yan, Phys. Rev. A **82**, 053407 (2010).
[37] P. K. Jha, H. Eleuch, and F. Grazioso, Opt. Commun. **331**, 198 (2014).
[38] H. Zimmermann, J. Buller, S. Eilzer, and U. Eichmann, Phys. Rev. Lett. **114**, 123003 (2015).
[39] See Supplemental Material at http://link.aps.org/supplemental/10.1103/PhysRevLett.128.173201 for (1) a definition of the pulse used in the theoretical work, (2) the analysis used to compare experimental and theoretical yields, including focal volume averaging and CEP noise, and (3) a description of the windowed FFT method used.
[40] X.-M. Tong and S.-I. Chu, Chem. Phys. **217**, 119 (1997).
[41] H. Li, V. A. Sautenkov, Y. V. Rostovtsev, M. M. Kash, P. M. Anisimov, G. R. Welch, and M. O. Scully, Phys. Rev. Lett. **104**, 103001 (2010).
[42] J. Venzke, R. Reiff, Z. Xue, A. Jaroń-Becker, and A. Becker, Phys. Rev. A **98**, 043434 (2018).
[43] M. J. Seaton, Rep. Prog. Phys. **46**, 167 (1983).
[44] M. Aymar, C. H. Greene, and E. Luc-Koenig, Rev. Mod. Phys. **68**, 1015 (1996).
[45] X. Gao, X.-Y. Han, and J.-M. Li, J. Phys. B **49**, 214005 (2016).
[46] X. Gao and X.-M. Tong, Phys. Rev. A **100**, 063424 (2019).
[47] H. Xu, N. Haram, D. Chetty, R. T. Sang, and I. V. Litvinyuk, J. Phys. B: At. Mol. Opt. Phys. **54**, 134005 (2021).